Remaining lifetime modeling using State-of-Health estimation

Abstract

Technical systems and system's components undergo gradual degradation over time. Continuous degradation occurred in system is reflected in decreased system's reliability and unavoidably lead to a system failure. Therefore, continuous evaluation of State-of-Health (SoH) is inevitable to provide at least predefined lifetime of the system defined by manufacturer, or even better, to extend the lifetime given by manufacturer. However, precondition for lifetime extension is accurate estimation of SoH as well as the estimation and prediction of Remaining Useful Lifetime (RUL). For this purpose, lifetime models describing the relation between system/component degradation and consumed lifetime have to be established. In this contribution modeling and selection of suitable lifetime models from database based on current SoH conditions are discussed.

Main contribution of this paper is the development of new modeling strategies capable to describe complex relations between measurable system variables, related system degradation, and RUL. Two approaches with accompanying advantages and disadvantages are introduced and compared. Both approaches are capable to model stochastic aging processes of a system by simultaneous adaption of RUL models to current SoH. The first approach requires a priori knowledge about aging processes in the system and accurate estimation of SoH. An estimation of SoH here is conditioned by tracking actual accumulated damage into the system, so that particular model parameters are defined according to a priori known assumptions about system's aging. Prediction accuracy in this case is highly dependent on accurate estimation of SoH but includes high number of degrees of freedom. The second approach in this contribution does not require a priori knowledge about system's aging as particular model parameters are defined in accordance to multi-objective optimization procedure. Prediction accuracy of this model does not highly depend on estimated SoH. This model has lower degrees of freedom.

Both approaches rely on previously developed lifetime models each of them corresponding to predefined SoH. Concerning first approach, model selection is aided by state-machine-based algorithm. In the second approach, model selection conditioned by tracking an exceedance of predefined thresholds is concerned. The approach is applied to data generated from tribological systems. By calculating Root Squared Error (RSE), Mean Squared Error (MSE), and Absolute Error (ABE) the accuracy of proposed models/approaches is discussed along with related advantages and disadvantages. Verification of the approach is done using cross-fold validation, exchanging training and test data. It can be stated that the newly introduced approach based on data (denoted as data-based or data-driven) parametric models can be easily established providing detailed information about remaining useful/consumed lifetime valid for systems with constant load but stochastically occurred damage.

Keywords: Structural health monitoring; wear aging; prognosis; feature extraction; state classification; remaining lifetime modeling; condition-based maintenance

---

1. Introduction

Technical systems operating under different, usually intermittent and hardly predictable, loading profiles undergo gradual degradation over time. Examination of degradation mechanisms and modes often entails an examination of materials rather than the system components. Moreover, different systems/materials exhibit different types of degradation. For instance, either gradual degradation of machining tool or sudden tool fracture or breakage occurs due to high operational load (like high pressures, strong fatigue loads) on machine components during the machining processes [1] [2]. However, gradual degradation of system ultimately leads to failure, whereas the failure is defined as a loss of functionality where the system is not capable to perform predefined tasks. Time point at which this happens is stated as end of service lifetime. From that point onwards the system becomes not anymore functional and has to be phased out of use. For diagnostic (and sometimes also for prognostics) purposes, the propagation of degradation over time is often continuously monitored [3] [4]. Benefits achieved by continuous monitoring of current systems degradation level are primarily reflected in timely performed maintenance and operation action targeting to avoid catastrophic

events (for instance: with life-threatening injuries of humans), or increased costs of repairment and operation actions if not done in right time. The benefit emphasized here is the possibility for service lifetime extension under the condition that the information about current level of system degradation is integrated in control strategy, so as the controller outputs are not generated solely on the basis of commonly based system parameters but also considers actual level of system degradation. For these purposes, the tasks to be solved are: i) estimation of degradation indicator, ii) tuning of controller, and iii) adaption of the operating conditions. In this contribution, degradation level is discussed in terms of State-of-Health (SoH) and Remaining Useful Lifetime (RUL) estimation, both of them describing aging of systems/materials in similar way. The degradation level in case of RUL is expressed percentually and denotes the lifetime remained up to failure occurrence. If discussed in reliability framework, Probability of Failure (P_f) function is used to express RUL. Concerning T as the moment in time of failure occurrence and t as expected (predefined) survival time, P_f is expressed as

$$P_f = P(T - t > x | T < t). \tag{1}$$

Regardless of parameters used to describe degradation level, the determination of the degradation level is a precondition for lifetime extension. Consequently, deployment of lifetime model establishing relationship between operating conditions (model input) and degradation parameter (here: RUL) is of high importance. Thus, a number of lifetime model approaches are proposed in literature whereas all models can be grouped in data-based, model-based, and experience-based approaches [1-10]. Whilst model-based approaches attempt to find mathematical description of degradation processes, data-based approaches typically rely on statistical and artificial intelligence methods such as Hidden Markov Models (HMM), Neural Networks (NN), Unscented Kalman Filtering (UKF), and similar. To reveal information about degradation, experience-based approaches take into consideration previous knowledge of processes occurred in the system integrating the same into the model. Inceptive steps towards systems lifetime determination using cumulative damage model are introduced in the work of Palmgren and Miner [5, 6]. Cumulative damage model requires the knowledge about the relation between nominal stress and the number of cycles endurable by system under the assumption that the stress is held constant. The effects resulting from the stress applied to a system whose amplitude lies below predefined material specific level (so-called endurance limit) are neglected. Moreover, the sequence of

stress appearance is not considered. It may be concluded, Palmgren-Miner rule has some shortcomings primarily reflected in aforementioned assumptions and model linearity. Due to this, some authors [7, 8] proposed modifications of Palmgren-Miner rule. Modifications introduced by Henry [7] and Marco and Starkley [8] considers adding nonlinearities to Palmgren-Miner model to adapt the same to a specific systems. Contrary to those deterministic models, research on lifetime models conducted recently is focused on stochastic models capable to describe stochastic nature of degradation process.

Remaining useful lifetime estimation based on Rainflow Counting Algorithm (RCA) and Palmgren-Miner rule is introduced in [9]. This approach is used to model thermomechanical fatigue of semiconductors whose application is found in a variety of technical systems: wind turbines, speed drives, electric vehicles, airplanes, and similar. Equivalent temperature is considered as input. The effect of decreased stress endurability of metals with increased temperature is considered. To extract information about equivalent temperature, the authors use existing temperature-dependent model based on continuously monitored power factor. By using proposed time-temperature-dependent model, better accuracy in RUL calculation of semiconductors is obtained.

Singleton et al. [10] compare performance of Kalman Filter (KF) and Extended Kalman Filter (EKF) in RUL estimation of bearings. Different features are extracted from measurements originating from experimental tests done under different operating conditions. Further, time- and time-frequency-based features (variance and entropy) are calculated and compared with respect to their suitability for prognostics. Presented results proves that the entropy is more capable to describe gradual damage progression especially in inceptive degradation phase. Moreover, obtained prediction accuracy using EKF is better than the accuracy obtained using KF.

Concerning limitations of model- and data-driven-based approaches reflected primarily as necessary knowledge about underlying physical processes and the dependency on training data sets. Pecht et al. [11] propose a fusion of both approaches to assess the RUL. The model deployed in [11] is adapted to RUL estimation of electronics-rich systems. Performance of introduced model is illustrated on an example of printed circuit board. To establish a model, the parameters capable to reveal systems State-of-Health are chosen. Obtained knowledge about underlying physical processes, consequently the detection of present anomalies is utilized in this step. Obtained SoH is further used

to select appropriate data-driven based model (here: physics-based model) to predict RUL. According to [11], proposed model yields satisfying results regarding timely performed fault detection, fault criticality determination, as well as RUL prediction of electronic assemblies. The model can be extended to other application fields.

In [12], the classification of prognostic models into probabilistic and non-probabilistic models is proposed. Additionally, the comparison between non-probabilistic models and self-proposed Wiener process-based model is carried out by means of RUL prediction efficiency. As that, degradation indicator is identified using Principal Component Analysis and modeled by Wiener process. Whilst probabilistic models rely to a large extent to a probability theory and concern degradation parameter (RUL) as a random variable, non-probabilistic models rely on observations and measurements captured from system. Multiple Linear Regression, Neural Networks, and physics-based models are taken as an example of non-probabilistic models and discussed in [12] with special emphasize to RUL prediction accuracy. In addition, Wiener, Gamma, and Brownian processes as an example of probabilistic models are stated, but are not discussed in detail. Complete analysis is done based on the data provided through 2008 PHM Data Challenge [13]. By comparison of non-probabilistic models with Wiener process-based model proposed in [12], it is shown that RUL prediction using Wiener process provides more accurate prediction in comparison with traditional lifetime modeling approaches. Possibility to use stochastic process modeling for RUL prediction as one of approaches towards lifetime modeling is thereby proved.

Further, detailed review of statistical data-driven approaches for systems lifetime estimation with special emphasize to recently developed ones is given in [14]. The models reviewed in [14] are generally divided into the models relying on directly observable states and models including non-directly observable states. As stated in [14], statistical data-driven approaches estimate RUL by fitting deployed statistical model to previous (past) data captured through condition monitoring system. These models rely on probabilistic models and do not consider underlying physical principles. The models taking in consideration directly observable states as discussed in [14] are regression-based models, Wiener process, Markovian-based models, and Gamma process. Contrary to these models, the models considering indirectly observable states as stated in [14] are stochastic filtering-based models, hazard models, Hidden Markov model, and Hidden semi-Markov model. According to authors, RUL modeling using models with hidden (not directly observable)

states are more complex due to complex relations between hidden and observed states, but are more closer to practical application as system states are often not directly accessible (measurable). Regardless of used statistical model, practical application is still aggravated and the further research is necessary.

Similarly, Wang et al. [15] infer RUL estimation of gearboxes using two health indicators extracted based on frequency spectrum of vibration signal. Both features (here stated as health indicators) are constructed using two Bayesian networks which are mutually independent. According to [15], early detection of fault using extracted health indicators is possible. Moreover, these features along with sequential Monte Carlo algorithm are further used to predict future State-of-Health of gearboxes and to obtain probability function of gearboxes failure. Using aforementioned probability function accurate RUL estimation is possible. Efficiency of proposed model is proved using experimental data from a gearbox accelerated tests.

It may be concluded from previous discussion that there are a number of different lifetime models developed over years. Those models have specific limitations and are not dependent on current SoH. Some models require a priori knowledge of underlying physical degradation processes, some of them are dependent on the quality of condition monitoring data to a large extent, show different model complexity, or faces problems with regard to practical application. This implies that existing models for RUL estimation are not adapted to current level of system's aging. An adaption of RUL models to current level of system's aging may contribute to lower prediction error and justifies the development of the two approaches developed in this contribution.

Primary contribution of this paper is the development of a new type of damage accumulation model applicable to tribological systems which integrates the knowledge (using measurements) about current State-of-Health in the model itself. First approach introduced in section 2 considers Acoustic Emission energy as input signal to the model, whilst the second one uses the cumulative sum of AE energy as model input. A detailed description of both models is given in section 2. Experimental test rig, obtained AE-based characteristic values, steps towards model validation, as well as discussion about obtained results are detailed in the third section. The contribution closes with summary and outlook.

2. Concept of SoH-based lifetime modeling

2.1. General overview

According to literature [12-19], different wear mechanisms and modes can be distinguished in tribological systems which exhibits sliding or rolling motion. Structural health monitoring of wear-susceptible systems can be performed using AE-based monitoring methods, as proposed in [21] or [23]. By wear examination in tribological system clear distinction between three different degradation phases are noticeable based on AE measurements: i) run-in phase, ii) permanent wear phase, and iii) wear-out phase [16].

In [16] and [17], a tribological system is considered establishing a new approach able to distinguish three different wear phases. As system measurements in [16] and [17], AE measurements are used. Based on AE measurements, specific frequency spectrum of AE signal corresponding to signal energy is used to distinguish different wear phases. At first glance, higher amplitudes of AE energy are evident at the very beginning and at the end corresponding to run-in and wear-out phase, respectively. Additionally, higher amplitudes are noticeable in some time periods between run-in and wear-out phases. The fact that different phases can be differentiated concerning energy of AE signal is utilized for lifetime model establishment and model parameter optimization. General overview of proposed concept is given in Figure 1. Based on the continuously measured AE signal using piezoceramic sensor a suitable feature extraction (here: using signal transformation in time-frequency domain) is realized. Using AE energy or integrated energy in combination of the trained lifetime model, RUL estimation can be done. The same data still can be used for Fault Detection and Isolation (FDI).

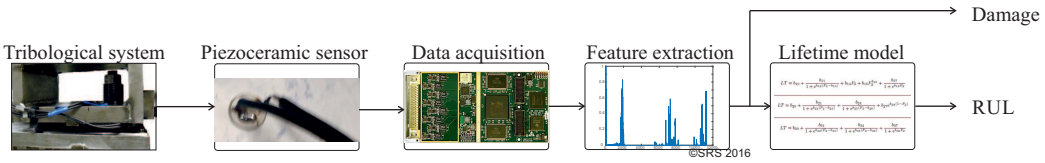

Figure 1: General overview

Model Type I. The first model proposed here relies on a state machine approach to establish relation between damage accumulated in the system and accompanying consumed lifetime. The state machine suggested here is based on four machine states whereas these four states can, but do not have to,

correspond to three different phases mentioned above. Each state as well as transitions from one state to another is defined according to a priori identified thresholds, illustrated as tr_1, tr_2, tr_3, and tr_{DIFF} (Figures 2 and 3). For this approach it is assumed that the thresholds are defined by experts. They are equal for different experiments. Based on one training example, the thresholds can be defined. The states are defined as follows: i) state S_1 is defined as the state with high changes in the system at the beginning of service lifetime (initial use of the system), ii) states S_2 and S_3 are the states with small and high changes in the system successively occurred between first use of the system and loss of functionality, and iii) state S_4 is a state characterized by loss of functionality.

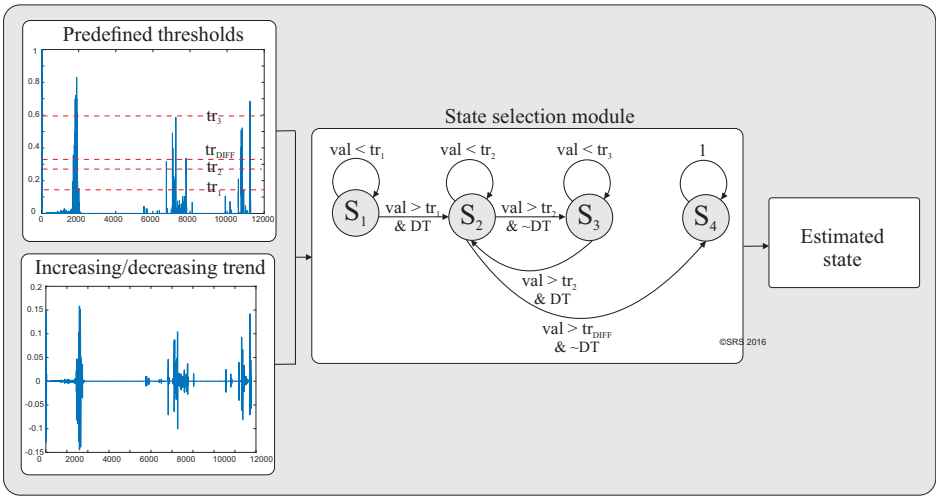

Figure 2: State selection according to predefined thresholds

Initial state is STATE 1, denoted as S_1 in Figure 2. Possible transition from state S_1 is only to state S_2 and occurs when the threshold tr_1 is exceeded and model input exhibits decreasing trend. Once state S_2 is reached, it is not possible to return to state S_1. Possible transitions from state S_2 are to states S_3 and S_4. If threshold tr_2 is exceeded and model input shows increasing trend, state S_3 is reached. Otherwise, if threshold tr_{DIFF} is exceeded showing simultaneously increasing trend of model input, state S_4 is reached. Once S_4 is reached, it is not possible to return to other states. State S_2 can be reached also from state S_3 in case that threshold tr_2 is exceeded and the decreasing trend of model input is detected. As long as the thresholds tr_1, tr_2, tr_3, and tr_{DIFF} are not exceeded, machine state would not be changed. In this case,

thresholds are fixed and are not used for optimization of model parameters.

Additionally, decreasing or increasing trend of input into the model is determined and utilized in machine state determination. Once the state is recognized, appropriate mathematical description of lifetime model is chosen to estimate consumed (remaining) lifetime. This simultaneously means that four different lifetime models, each of them corresponding to one machine state, have to be deployed.

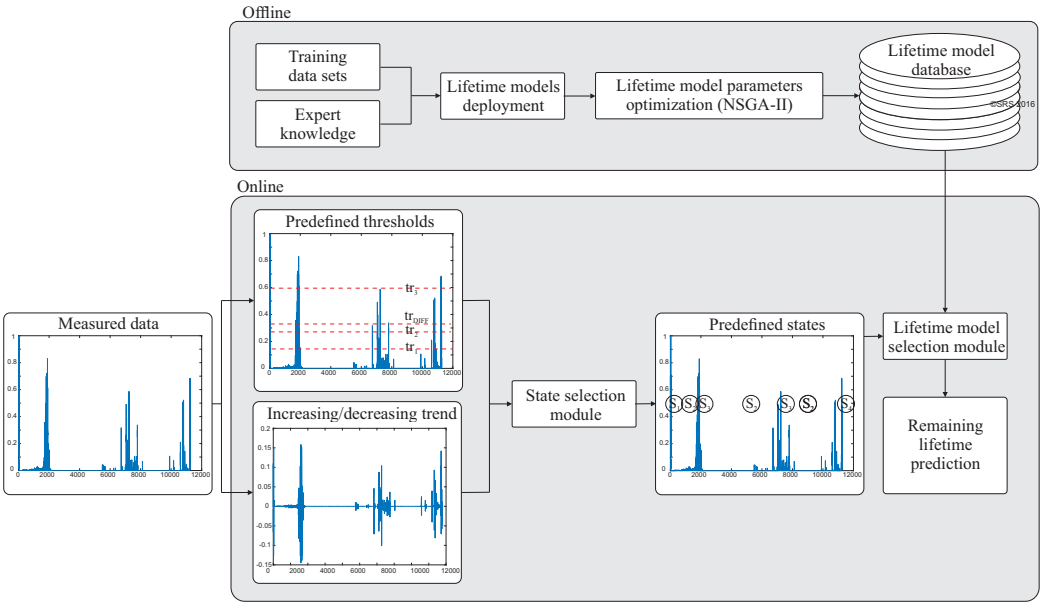

Figure 3: Concept of SoH-based lifetime modeling using lifetime model selection based on actual machine state

Mathematical formulation used to describe relation between degradation parameter and consumed (or remaining) lifetime valid for particular state is identical in all four states, but the parameters accompanied to the model are not the same. As that, the same functional form models relation between degradation parameter and consumed (or remaining) lifetime, but model parameters have to be optimized for each particular state individually, as listed in Table 1. Parameters to be optimized according to recognized machine state are a_{x0}-a_{x8}, where x denotes a particular machine state. Accordingly, four different states require the optimization of 36 model parameters, which means 9 parameters per state. Mathematical equations describing aforementioned relations are listed in 3.

TABLE 1: Mathematical formulations of lifetime models for *Model Type I* (based on [25])

STATE 1	$LT = a_{10} + \frac{a_{11}}{1+e^{a_{12}(F_1-a_{13})}} + \frac{a_{14}}{1+e^{a_{15}(F_1-a_{16})}} + \frac{a_{17}}{1+e^{a_{18}F_1}}$
STATE 2	$LT = a_{20} + \frac{a_{21}}{1+e^{a_{22}(F_1-a_{23})}} + \frac{a_{24}}{1+e^{a_{25}(F_1-a_{26})}} + \frac{a_{27}}{1+e^{a_{28}F_1}}$
STATE 3	$LT = a_{30} + \frac{a_{31}}{1+e^{a_{32}(F_1-a_{33})}} + \frac{a_{34}}{1+e^{a_{35}(F_1-a_{36})}} + \frac{a_{37}}{1+e^{a_{38}F_1}}$
STATE 4	$LT = a_{40} + \frac{a_{41}}{1+e^{a_{42}(F_1-a_{43})}} + \frac{a_{44}}{1+e^{a_{45}(F_1-a_{46})}} + \frac{a_{47}}{1+e^{a_{48}F_1}}$

Changes in consumed lifetime are denoted as LT and extracted feature (in this case measured operation parameter) as F_1. The determination of optimal values of unknown model parameters is performed using Non-dominated Sorting Genetic Algorithm (NSGA-II). The optimization algorithm is used in the application to define unknown model parameters by optimization. Non-dominated Sorting Genetic Algorithm is used in its original form proposed by Song [24].

The algorithm used here is a sort of Genetic Algorithms (GAs). The approach provides simultaneous optimization for more than one objective function. By comparing GA with NSGA-II, it is worth to emphasize that so-called pareto non-dominated fronts using NSGA-II are formed of best ranked individuals, whereas the ranking is done based on euclidean distance. Defined objective functions here are closely related to the minimization of discrepancies between experimental and estimated data sets. Model parameters are considered as a population of NSGA-II, whilst different values of model parameters provide different trade-off between defined objectives. As that, the objectives are seen as conflicting objectives and the optimization of model parameters can be carried out using NSGA-II. Further details are given in [24].

Features utilized for optimization of model parameters as well as for model validation are explained in detail in the next section.

Model Type II. Conversely to the modeling approach introduced in previous section where the selection of lifetime model is conditioned by machine state recognition, the model selection concerning *Model Type II* is based

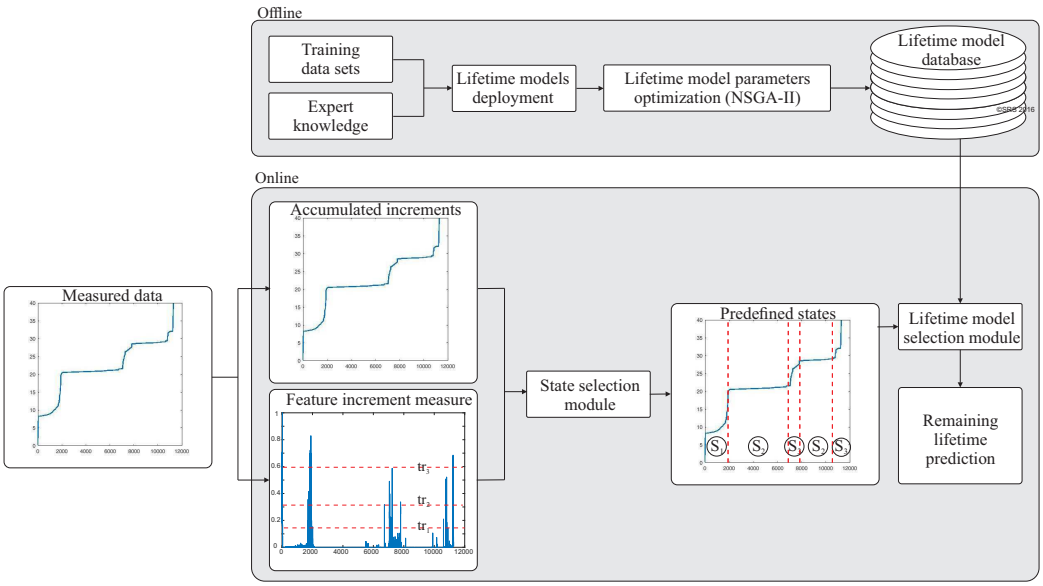

Figure 4: Concept of State-of-Health-based lifetime modeling by tracking predefined thresholds exceedance

primarily on appropriate feature extraction and an included thresholds optimization. According to optimized thresholds and differential of extracted features showing its increments, three different behaviors i, ii, and iii are modeled. Here, i) denotes no significant change in lifetime consumption, ii) denotes noticeable, but not significant change in lifetime consumption, and iii) denotes significant change in lifetime consumption. Here, aforementioned states are defined in accordance to the behavior observed in practice. Contrary to *Model Type I* where thresholds are fixed and not concerned in model parameters optimization, here the optimization of thresholds is considered as the thresholds are integral part of the model. Accordingly, optimized model parameters obtained using NSGA-II are the thresholds of *Model Type II* and they are the same for different experiments. Extracted features have to be capable to reflect monotonically increasing character of the degradation as lifetime model selection is based solely on threshold exceedance (Figure 4).

Accordingly, the relation between degradation parameters and consumed (or remaining) lifetime cannot be modeled using the same functional form. Therefore, different mathematical formulations have to be chosen. Mathematical relations are listed in Table 2. Particular mathematical model is selected in accordance with predefined threshold exceedance. As already

TABLE 2: Mathematical formulations of lifetime models for *Model Type II*

WITHOUT SIGNIFICANT CHANGE	$LT = b_{10} + \frac{b_{11}}{1+e^{b_{12}(F_2-b_{13})}} + b_{14}F_2 + b_{15}F_2^{b_{16}} + \frac{b_{17}}{1+e^{b_{18}F_2}}$
NOTICEABLE, BUT NOT SIGNIFICANT CHANGE	$LT = b_{20} + \frac{b_{21}}{1+e^{b_{22}(F_2-b_{23})}} + \frac{b_{24}}{1+e^{b_{25}(F_2-b_{26})}} + b_{27}e^{b_{28}(1-F_2)}$
SIGNIFICANT CHANGE	$LT = b_{30} + \frac{b_{31}}{1+e^{b_{32}(F_2-b_{33})}} + \frac{b_{34}}{1+e^{b_{35}(F_2-b_{36})}} + \frac{b_{37}}{1+e^{b_{38}F_2}}$

pointed out, thresholds are defined by using NSGA-II optimization algorithm, so that the thresholds as well as model parameters are simultaneously optimized. Model parameters to be optimized are b_{x0}-b_{x8}, while are b_{x9}-b_{x12} are thresholds accompanied to aforementioned changes of consumed lifetime (tr_1, tr_2, tr_3, tr_{DIFF}). Similarly, LT denotes changes in consumed lifetime and F_2 denotes extracted feature capable to describe monotonical increase of degradation indicator over time. Features F_2 utilized for optimization of model parameters and validation are explained in detail in the next section.

3. Experimental validation

3.1. Experimental setup and monitored system variables

As already stated in section 2, experimental data sets are required for lifetime model training and validation. For purpose of wear examination in a concrete tribological system, operation variables to be used for model training and validation, namely measurements gathered through continuous health state monitoring, have to be capable to describe wear effects. In the tribological system (depicted in Figure 5 and setted up at the Chair of Dynamics and Control, University of Duisburg-Essen) two operation variables are used as variables capable to reveal wear initiation and propagation: hydraulic pressure and Acoustic Emission [16, 17]. Any of these two variables/measurements captured from real system can be used as training or validation data sets as both of them describe in similar way occurred tribological effects in the system. In this contribution, only AE measurements are used.

The system consists of two metallic plates sliding against each other. Surface areas of plates are not the same but are in ratio 1:5. The plate with

larger surface area is fixed and performs no movement, whilst the plate with smaller surface area performs linear movements. The plate is driven by hydraulic cylinder whereas the movement trajectory is in advance planned and programmed. This means, the plate moves forward and backward in exactly predefined time intervals. The movement is performed in time interval of 40 s followed by an idle time of 70 s, which is considered as one cycle. As may be seen in Figure 5, normal force is applied targeting to accelerate aging. The test are done under variable friction and lubrication conditions.
Tribological system is equipped with a set of sensors. For purpose of RUL estimation, AE measurements are utilized. Acoustic Emission waves are measured using a piezoelectric sensor. It is important to emphasize that AE signal is a signal of low amplitude whereas frequency bandwidth in which AE signal appears covers frequency bandwidth up to 1 MHz. Due to this, measurement chain consist of preamplifier and FPGA-module with integrated high-frequency A/D converters, as depicted in Figure 5. Such measurement chain provides possibility for capturing continuous AE signal. It should be noted that this approach is not based on counts, peaks, or similar facts typical for AE-based measurements. Those measurements are used in this case alongside appropriate signal processing technique to reveal damage in the system. Short-Time Fourier Transformation (STFT) is applied to continuous AE signal, so that the obtained values correspond to each cycle (explained above). Here, the energy of AE signal corresponding to a particular cycle is obtained. Only one characteristic value for a given cycle representing energy of AE signal is calculated. The dependencies and variations of piezoceramic sensor coupling on quality of captured AE data is not examined. Conversely, for measuring hydraulic pressure no amplifier or specific measurement chain is required.

Features of AE signal are further used as input to lifetime model: for the first model energy of AE signal, and for the second model cumulative sum of energy of AE signal is used. Here, energy of AE signal per cycle is understood as damage increment whereas accumulated damage is defined as a cumulative sum of damage increments.

3.2. Experimental results

Four data sets, namely Z15, Z20, Z21, and Z24, obtained from tests conducted under different operating conditions are used as training data sets, whilst two additional data sets are used for model evaluation, Z22 and Z16. The same training/evaluation data sets are used within both proposed

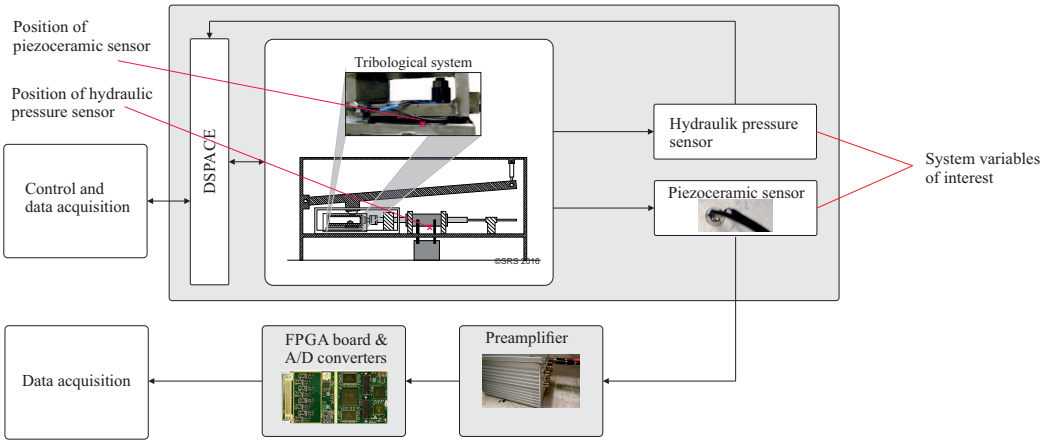

Figure 5: Test rig for wear examination, Chair of Dynamics and Control, SRS, U DuE

models. Concerning *Model Type I* characteristic values of AE energy are used as input into the model and corresponds to F_1 in the equations listed in Table 1. Taking in consideration *Model Type II*, not characteristic values of AE energy but their cumulative sum is used as an input. Cumulative sum of AE energy corresponds to F_2 in the equations listed in Table 2.

Model Type I. Values of previously listed parameters in Table 1 after optimization procedure is performed, are given in Table 3. Experimental and estimated data sets are compared in Figure 6. Training data sets (Z21, Z22, Z15, and Z20) and accompanying experimental and estimated values of lifetime are shown in the upper plot of Figure 6. Similarly, model validation using validation data sets (Z16 and Z24) is depicted in the lower plot of Figure 6.

TABLE 3: Optimized parameters of *Model Type I*

	a_{x0}	a_{x1}	a_{x2}	a_{x3}	a_{x4}	a_{x5}	a_{x6}	a_{x7}	a_{x8}
STATE 1	-0.122	0.247	-0.202	0.143	0.023	0.06	-0.310	-0.018	0.084
STATE 2	0.173	-0.178	0.365	-0.200	-0.039	-0.034	0.05	-0.16	0.315
STATE 3	0.075	0.21	0.263	0.113	-0.113	0.333	-0.122	-0.055	0.085
STATE 4	-0.084	0.298	-0.168	-0.103	-0.285	-0.384	0.014	0.155	-0.414

Model Type II. Values of optimized model parameters, which are previously listed in Table 2, are given in Tables 4 and 5. Comparison of experimental and estimated data sets is illustrated in Figure 7. Similarly as for *Model Type I*,

training data sets (Z21, Z22, Z15, and Z20) and accompanying experimental and estimated values of lifetime are shown in the upper plot of Figure 7, whereas validation results for Z16 and Z24 are shown in lower plot of Figure 7.

TABLE 4: Optimized parameters of *Model Type II*

	b_{x0}	b_{x1}	b_{x2}	b_{x3}	b_{x4}	b_{x5}	b_{x6}
WITHOUT SIGNIFICANT CHANGE	-176 10e-5	3 10e-5	92 10e-5	103 10e-5	4 10e-5	67 10e-5	-207 10e-5
NOTICEABLE, BUT NOT SIGNIFICANT CHANGE	12 10e-5	-57 10e-5	165 10e-5	-170 10e-5	71 10e-5	166 10e-5	75 10e-5
SIGNIFICANT CHANGE	85 10e-5	100 10e-5	-253 10e-5	-208 10e-5	-236 10e-5	-254 10e-5	255 10e-5

TABLE 5: Optimized parameters of *Model Type II*

	b_{x7}	b_{x8}	tr_1	tr_2	tr_3	T_{DIFF}
WITHOUT SIGNIFICANT CHANGE	248 10e-5	-162 10e-5				
NOTICEABLE, BUT NOT SIGNIFICANT CHANGE	142 10e-5	-301 10e-5	0.5988	0.6931	0.5903	0.9094
SIGNIFICANT CHANGE	-300 10e-5	-108 10e-5				

In Table 4, thresholds noted as tr_1, tr_2, tr_3, and t_{DIFF} are correlated to differential of cumulative sum of AE energy, whereas threshold tr_{DIFF} is used to indicate that the change has even happened.

3.3. Discussion about obtained results

Root Squared Error (RSE), Mean Squared Error (MSE), and Absolute Error (ABE) are used as performance criteria to compare efficiency of two proposed approaches/models. Some other criteria can also be used to obtain a measure of model accuracy, but here the focus is set to RSE, MSE, and ABE. Root Squared Error, Mean Square Error, and Absolute Error are defined as

TABLE 6: RSE, MSE, and ABE measures obtained using validation data sets

	RSE	MSE	ABE
Z16 - *Model Type I*	67.1641	0.0924	12167
Z16 - *Model Type II*	120.8769	0.2992	21169
Z24 - *Model Type I*	101.7152	0.2119	21704
Z24 - *Model Type II*	142.6347	0.4166	20679

$$
\begin{aligned}
RSE &= \sqrt{\sum_{n=1}^{n} (estimated \quad value - experimental \quad value)^2}, \\
MSE &= \sum_{n=1}^{n} \frac{(estimated \quad value - experimental \quad value)^2}{n}, \\
ABE &= \sum_{n=1}^{n} |estimated \quad value - experimental \quad value|,
\end{aligned}
\tag{2}
$$

respectively. Concerning proposed two modeling approaches and two validation data sets (not training data sets), RSE, MSE, and ABE are calculated and the results are listed in Table 6. A detailed look at Table 6 reveals that the results obtained using (*Model Type I*) are slightly better in comparison with the results obtained using (*Model Type II*).

According to Figures 6 and 7, it is noticeable that the deviation between estimated and experimental data sets is not high. Small deviation obtained concerning validation data sets as well as calculated error metrics prove the efficiency of both proposed models to establish a relation between measured (operation) variables and degradation related indicators (for instance: damage increments).

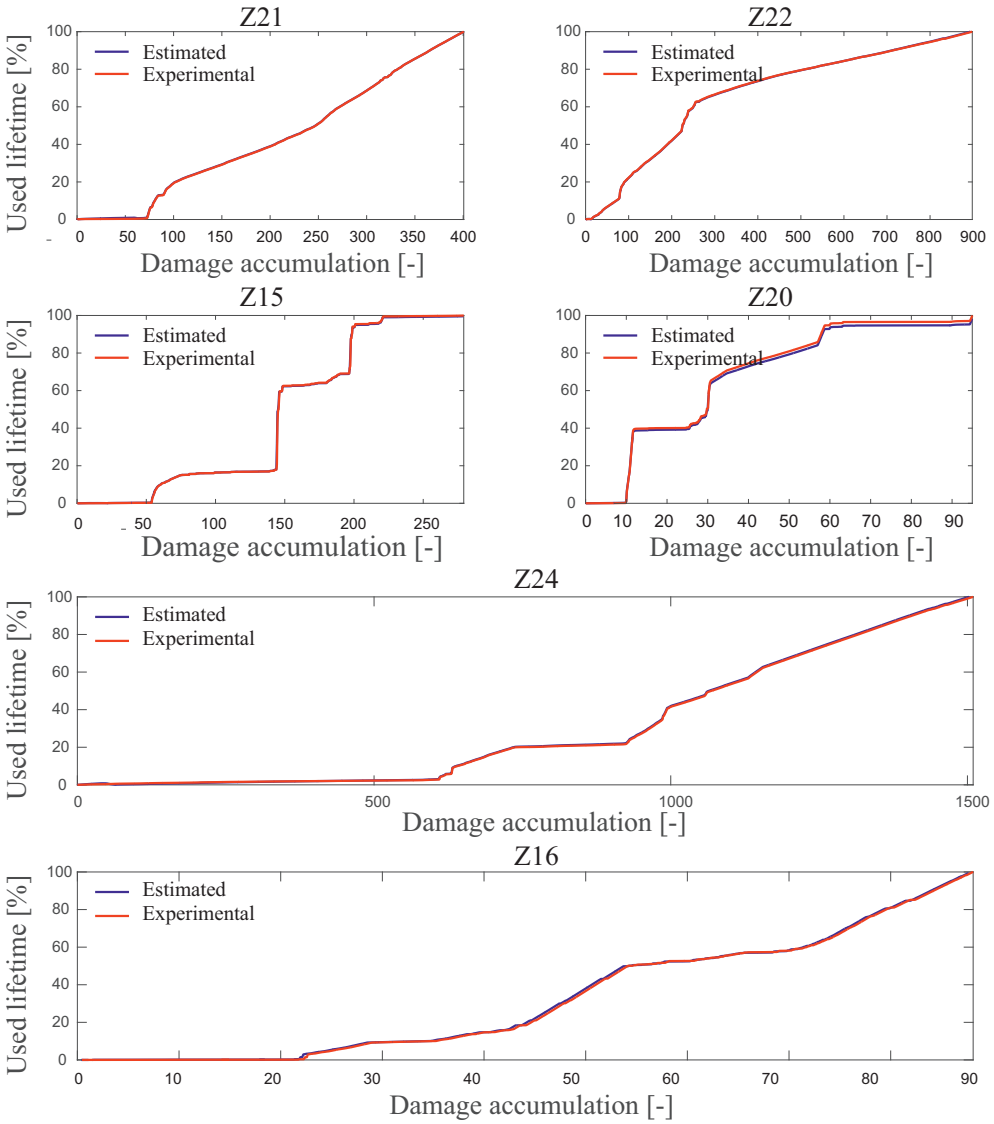

Figure 6: Experimental and estimated service lifetime using *Model Type I*: Upper four plots - training datasets; lower two plots - validation datasets

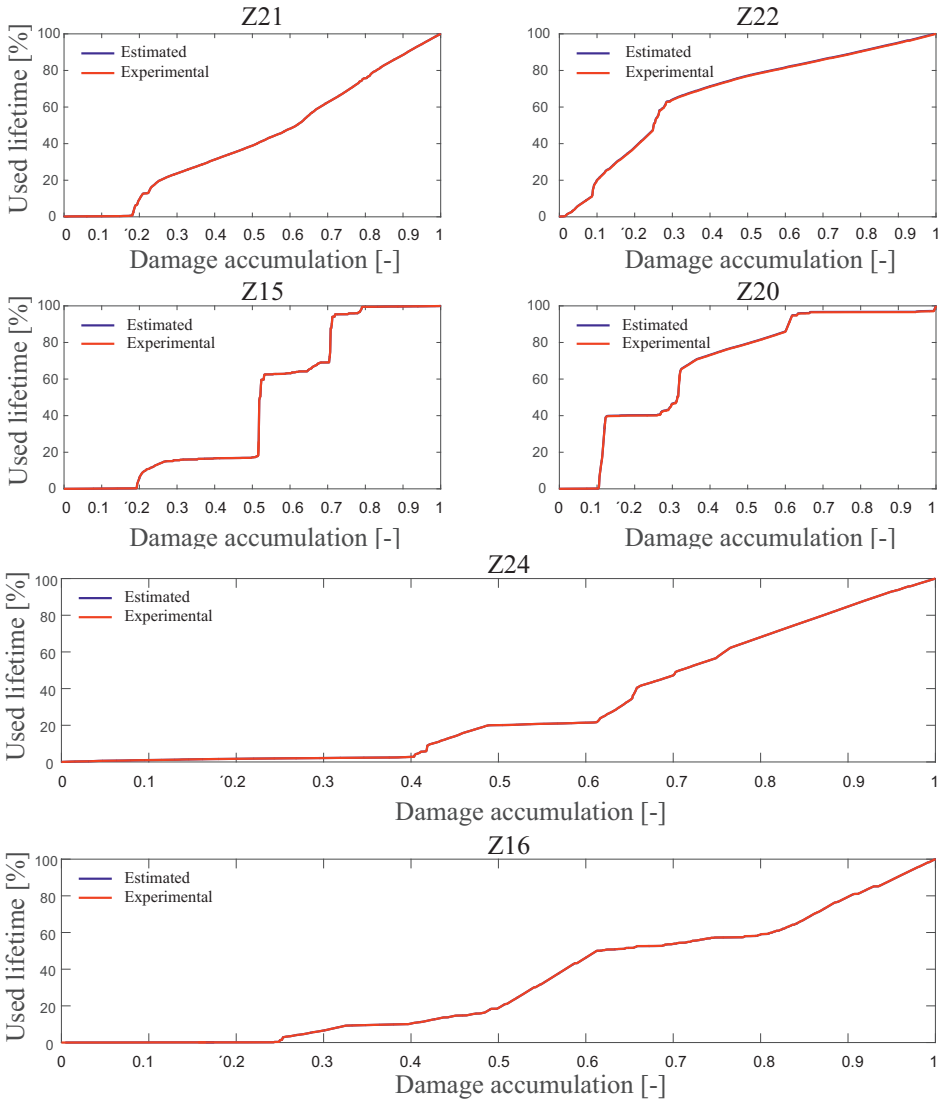

Figure 7: Experimental and estimated service lifetime using *Model Type II*: Upper four plots - training datasets; lower two plots - validation datasets

In addition, a detailed analysis based on an identical metrics is carried out with special emphasis to model applicability to lifetime prognosis. In these terms, it would be assumed that not all incomes of measured operation variables are available (as it is case in practice if the system is still functional). Number of assumed available incomes is given in percentages of all incomes and varied in steps of 10%. Accordingly, 10%, 20%, 30%, 40%, 50%,

60%, 70%, and 80% of available incomes are considered. For prognosis purposes, incomes which are not available are considered as constant and equal with respect to the last available income. In Figure 8 two different cases describing experimental test Z16 are illustrated. The two cases compare the results using 40% and 80% of incomes. It can be seen that the accumulated damage over the complete service lifetime for Z16 equals to 90. In detail, this means that 40% of all incomes are incomes obtained between 0 and 36 of accumulated damage (red line), whereas 80% of all incomes are incomes obtained between 0 and 72 of accumulated damage (blue line). Based on this approach, it is assumed that there are no more changes in damage increments. This case is rarely if ever seen in practice, but still can be utilized for model evaluation and examination of its applicability for prognosis purposes.

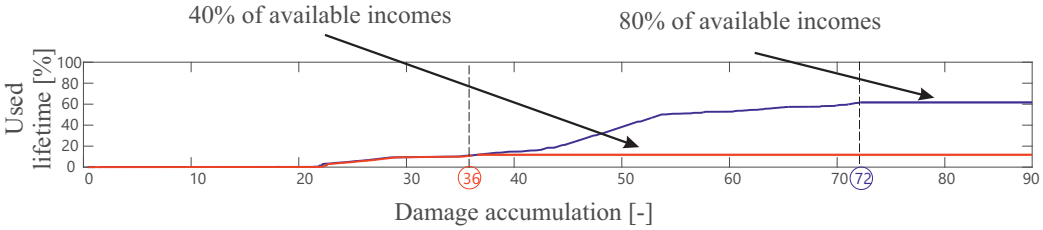

Figure 8: Graphical illustration of an assumption that only a number of incomes of Z16 are available: accumulated damage over complete service lifetime is 90, considered available incomes: 40% and 80% of all incomes up to the EoL (red and blue line, respectively), all incomes beyond 40% and 80% of all incomes held constant

Obtained results concerning varying number of available incomes applied to both models and both evaluation data sets are depicted in Figures 9, 10, 11, and 12. According to presented results, there is no significant impact of number of available incomes to estimated consumed lifetime, briefly: the estimation procedure is able to estimate the lifetime from the very beginning (20 % of expected life time). 'Available incomes' denote the amount of data used for estimation of the upcoming lifetime behavior. As example the meaning of 30% of available incomes is that 30% of the data are used to estimate the used lifetime behavior for the period of useful lifetime from 31 to 100% and therefore predict the End-of-Lifetime (100%), which is by definition equal to D=1.

Using *Model Type I*, this can be explained as: i) machine state catched up at the time after which the increment is considered constant is real (expected) machine state of the majority of the next, currently unavailable,

incomes, and ii) machine states 1, 3, and 4 are similar and can in turn be modeled using similar mathematical model. If damage increments are held constant, machine state would also be held constant and possibly not correctly recognized. Even machine state is not correctly recognized, it would be compensated by a model. If this is not the case (for instance in Figure 10), second plot (20% of available incomes)), prognostic error would be high.

Similar situation concerning *Model Type II* can be justified as: i) state change is rarely occurred due to high threshold t_{DIFF} (0.9094 of 1, Table 5), and ii) only if high change in damage increment is detected (above 0.9094), the state would be changed. This means, aforementioned relations would often be modeled using only one mathematical equation (Table 2). It has to be emphasized, that threshold t_{DIFF}, preventing state change when not necessary, is optimized using NSGA-II as threshold t_{DIFF} is an integral part of the model. Additionally to the results shown in Figures 9, 10, 11, and 12, RSE, MSE, and ABE are calculated for each above mentioned case and presented in Table 7.

Detailed insight into the results shown in Table 7 reveals that the results obtained using *Model Type I* are in general slightly better than those obtained using *Model Type II*. Despite the fact that the results obtained using *Model Type II* are not as precise as those obtained using *Model Type I*, the results obtained using *Model Type II* show monotonical trend and have no sudden high peaks of values (what is equal to sudden higher prediction error) as it is the case with the results obtained using *Model Type I* (red marked values in Table 7). The deviation between estimated and real lifetime in dependence of the number of available incomes is depicted in Figure 13. No significant impact in this case is noticeable.

TABLE 7: Statistical variables concerning varying number of available incomes of Z24

Available incomes	RSE - Z16 *	MSE - Z16 *	ABE - Z16 *	RSE - Z24 *	MSE - Z24 *	ABE - Z24 *
10%	31.7/232.23	0.0206/1.105	6227/44693	112.2/182.5	0.2578/0.6826	23199/33942
20%	69.9/144.3	0.1/0.426	12612/28809	704.3/129	10.1/0.341	125267/24461
30%	70.1/115.54	0.1/0.273	12643/23720	78.5/29.92	0.126/ 0.018	16832/5640
40%	70.1/92.64	0.1/0.175	12637/19560	69.17/43.39	0.098/0.0385	14137/7829
50%	70.07/77	0.1/0.122	12628/16412	106.7/76.20	0.233/0.118	22638/12721
60%	67.5/91.2	0.0933/0.1705	12216/17440	92.04/103.5	0.1734/0.219	19831/16370
70%	67.1/106.5	0.092/0.2326	12162/19604	101.4/122.6	0.21/0.308	21655/18637
80%	67.2/115.1	0.092/0.2714	12179/20605	101.5/135.9	0.211/0.3786	21672/20055

* First values presented in table cells are obtained using *Model Type I*;
second values presented in table cells are obtained using *Model Type II*.

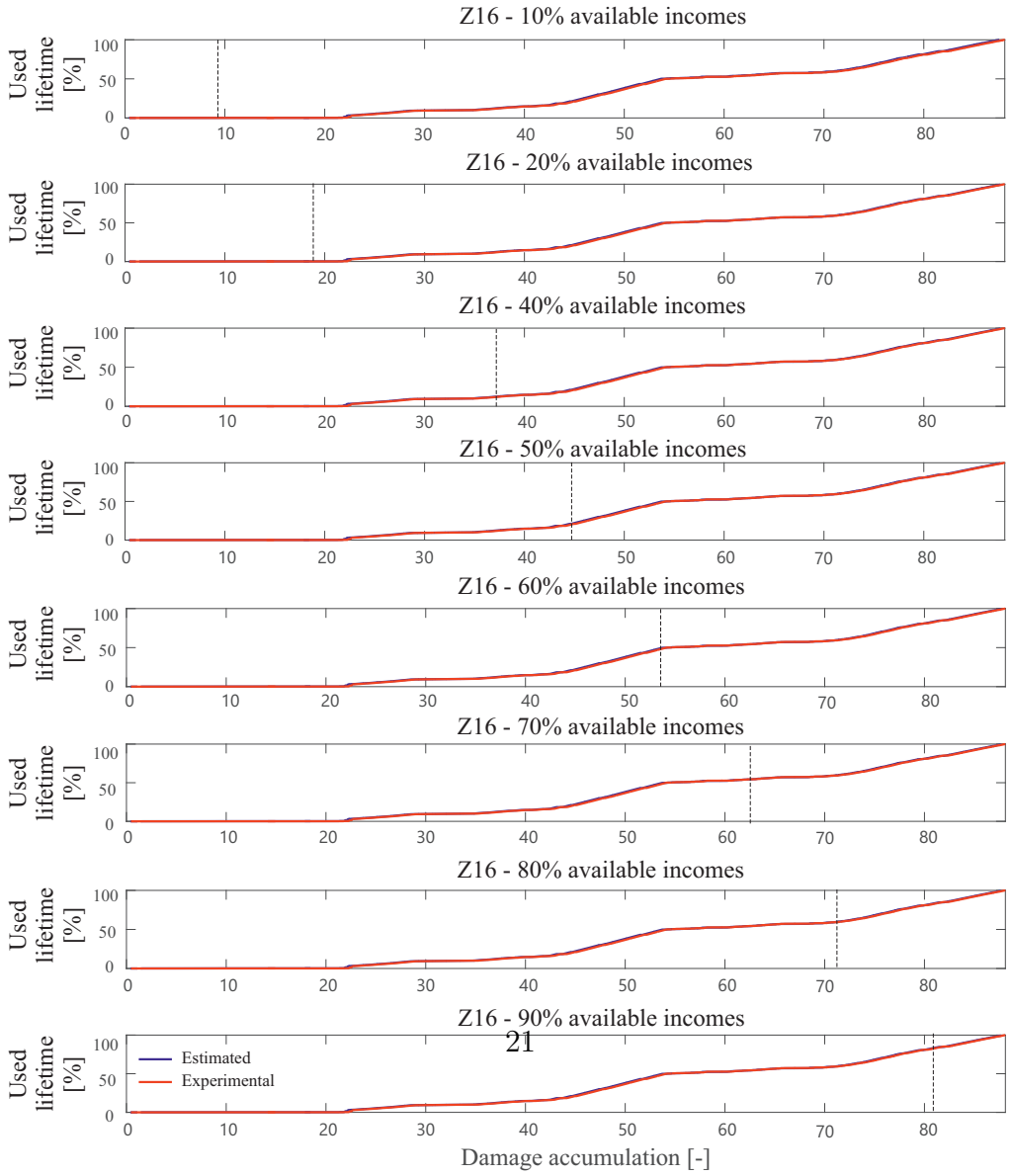

Figure 9: Lifetime prognostics using *Model Type I*: Available number of incomes varies (Z16)

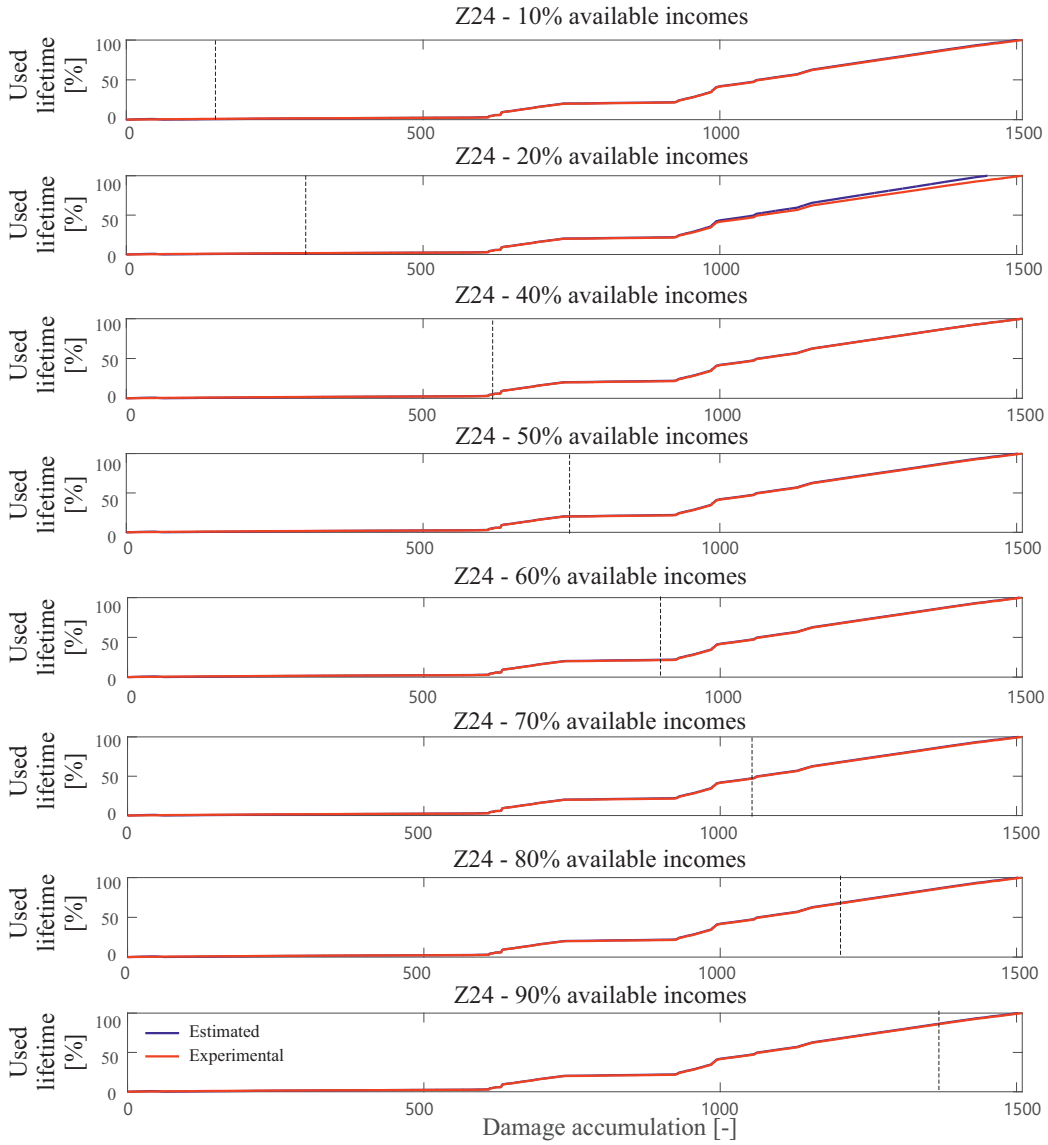

Figure 10: Lifetime prognostics using *Model Type I*: Available number of incomes varies (Z24)

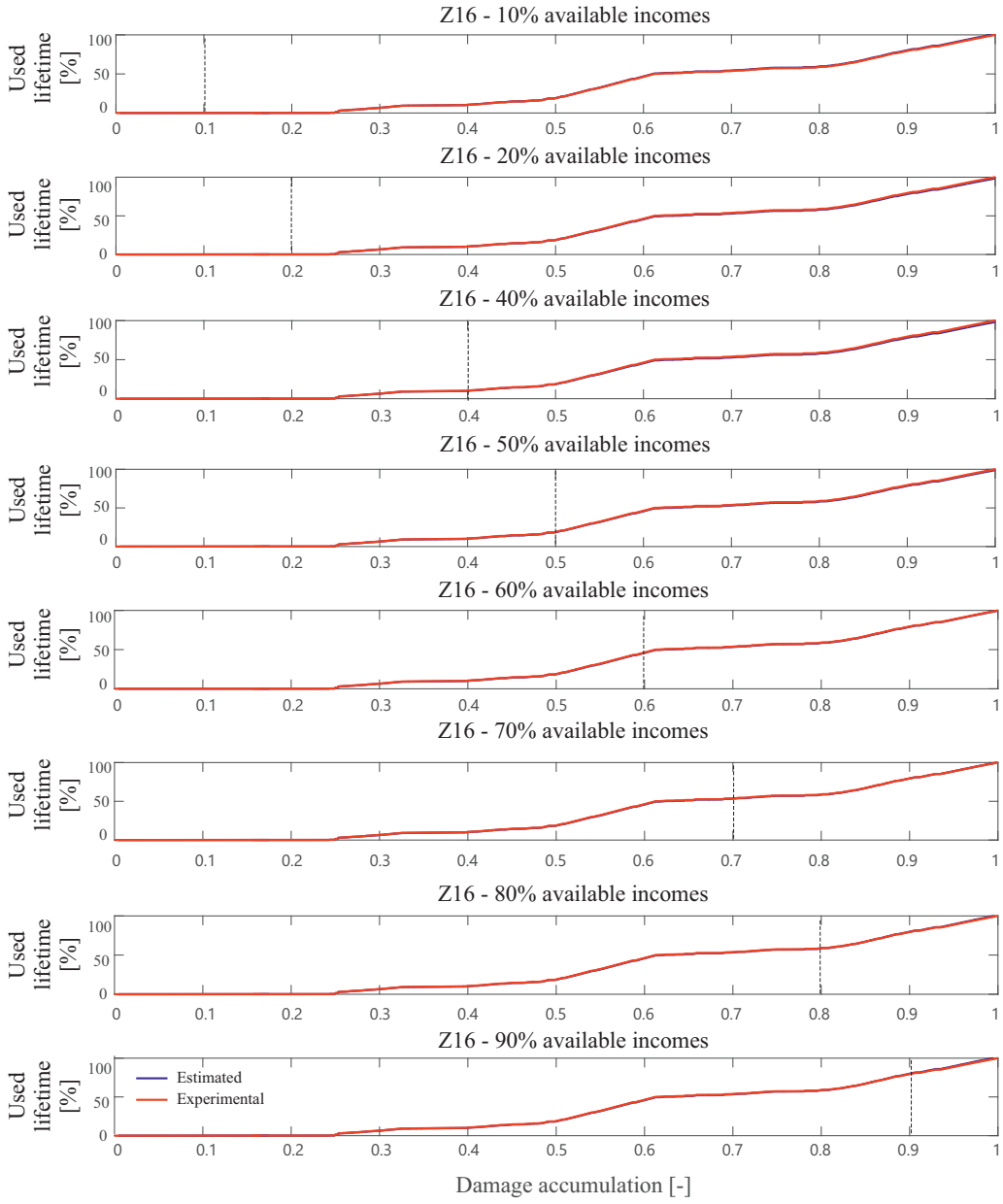

Figure 11: Lifetime prognostics using *Model Type II*: Available number of incomes varies (Z16)

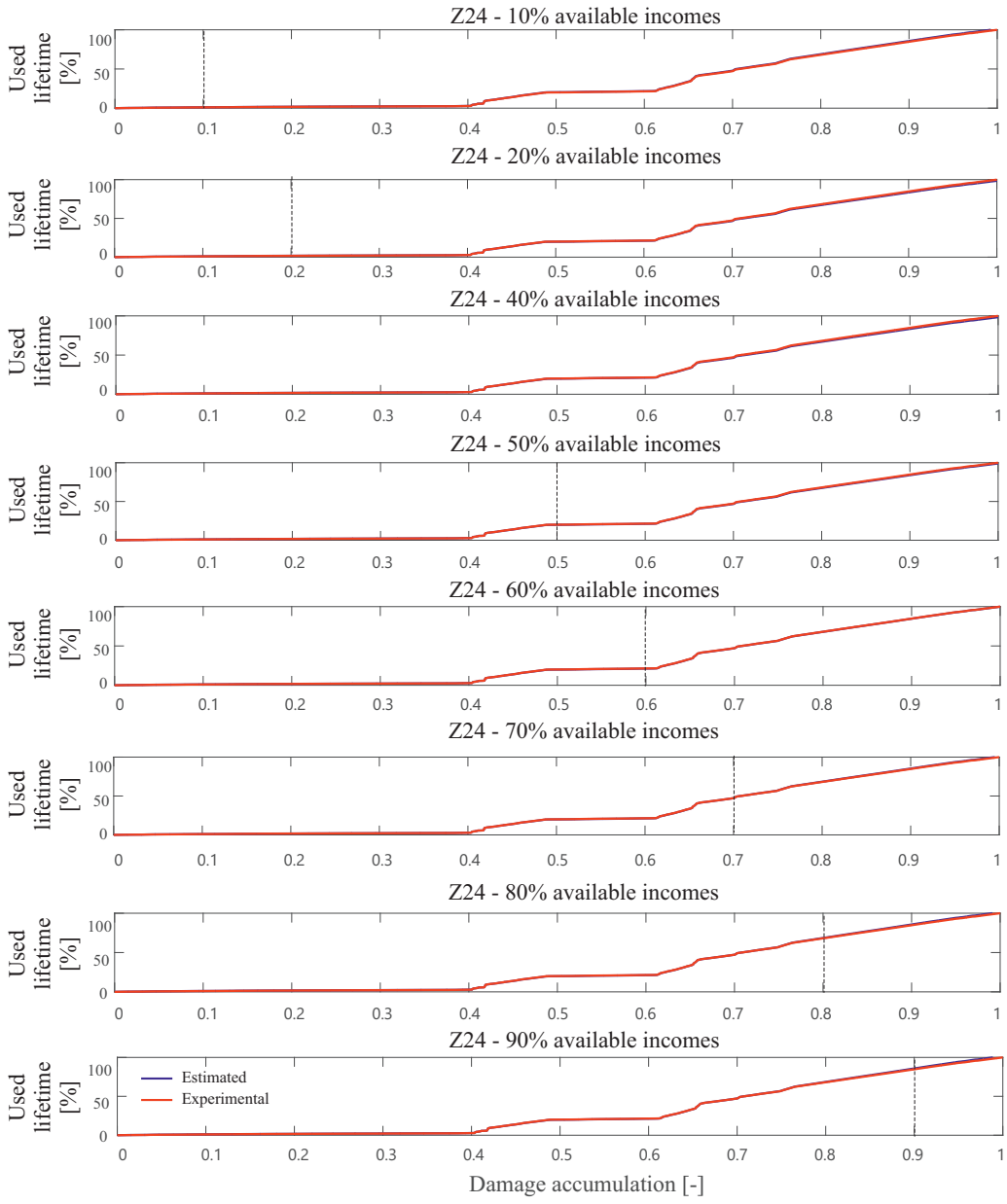

Figure 12: Lifetime prognostics using *Model Type II*: Available number of incomes varies (Z24)

TABLE 8: Selection of different groups of available data sets for model parameter optimization

Data set Test run	Z15	Z16	Z21	Z22	Z24	Z20
1	Training	Test	Training	Training	Test	Training
2	Test	Test	Training	Training	Training	Training
3	Training	Training	Test	Test	Training	Training
4	Test	Training	Training	Test	Training	Training
5	Test	Training	Training	Training	Test	Training
6	Training	Training	Test	Training	Training	Test

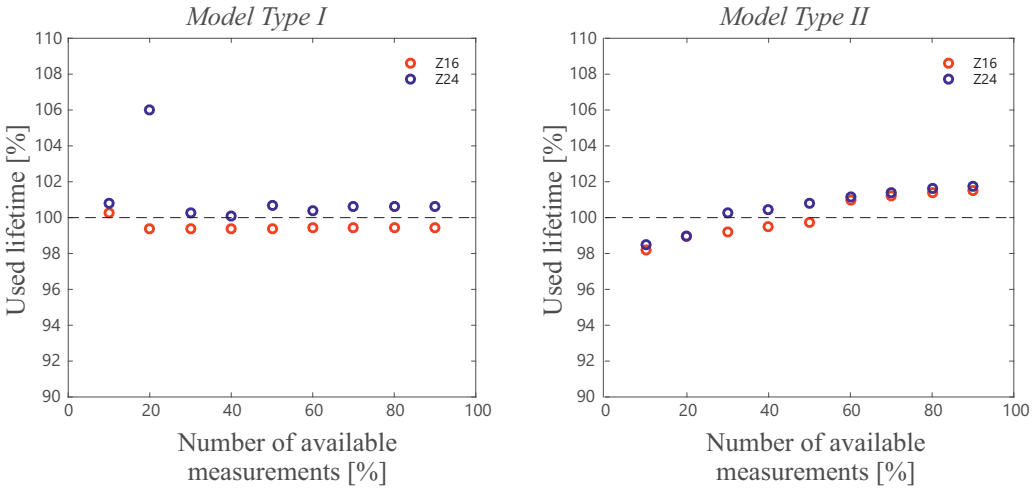

Figure 13: Prediction of End-of-Lifetime concerning different number of available measurements obtained using *Model Type I* and *Model Type II*

The effects by using different groups for training and test to generate the model parameters are shown in Figure 14. Groups of particular data sets used for model training or evaluation are given in Table 8. Here, six groups are chosen. The prediction of End-of-Lifetime estimation under the assumption that varying number of incomes are available is discussed. From Figure 14 it can be concluded that estimated and experimental EoL are found in the limits of +/-4% for *Model Type I* and +/-7% for *Model Type II*. It can be stated the results are independent from the data sets used for training and test. Using simple fold cross-validation approach, the results are not affected (as shown graphically).

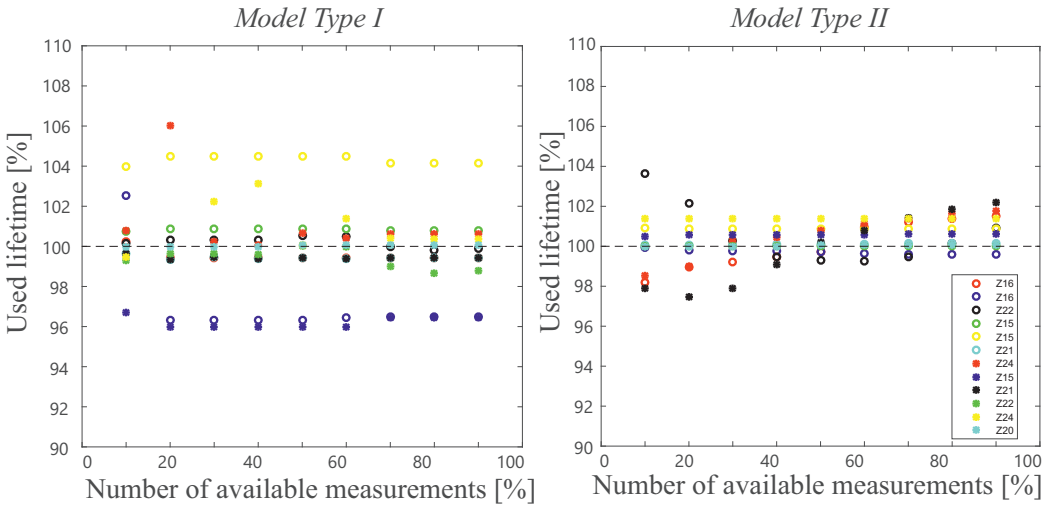

Figure 14: Prediction of End-of-Lifetime concerning different number of available measurements organized by an n-Fold training and test data set variation using*Model Type I* and *Model Type II*

Both proposed models also have limitations. If evident changes are present in measured data, proposed models provide high efficiency concerning prognostic purposes due to higher probabilities for accurate State-of-Health detection and higher sensitivity of the model to sudden changes occurred in the system. A lack of noticeable changes in measurement data lead to ambiguous State-of-Health determination and consequently to higher prediction error. If no evident changes are present, it is difficult to detect state changes (*Model Type I*) or optimize thresholds (*Model Type II*) what lead to higher prediction errors (Figure 14).

4. Summary and conclusion

A novel consumed (remaining) lifetime modeling strategy is introduced in this paper. Conversely to previous modeling approaches reviewed in section 1, a multi-stage model is proposed to consider different current states of health status of the system to be observed. State-of-Health in *Model Type I* is concerned through lifetime model selection using state-machine-based selection module, whereas the same is in *Model Type II* obtained through thresholds optimization according to current value of accumulated damage. Obtained results including simple fold cross-validation prove the capability of models to describe the relation between system degradation and system's

lifetime. Root squared error, mean squared error, and absolute error are used as performance criteria for both proposed models. The models are deployed using experimental data (energy of Acoustic Emission signal). Applicability of the models is illustrated on the data obtained from the tribological system. Here, contact partners perform sliding motion under exactly predefined operation conditions. These models can also be adapted to other application fields, such as for the lifetime prediction of machining tools whereas the change in mechanical properties of the material have to be described using lifetime models.
As an outlook, further examination on increased number of available experimental data sets can be done. This will primarily enable correlation of particular models to particular operation conditions.

References

[1] Ulutan D, Ozel T. Machining induced surface integrity in titanium and nickel alloys: A review. International Journal of Machine Tools and Manufacture 2011, 51(3): 250-280.

[2] Zhu D, Zhang X, Ding H. Tool wear characteristics in machining of nickel-based superalloys. International Journal of Machine Tools and Manufacture 2013, 64: 60-77.

[3] Zhu K, San WY, Hong GS. Wavelet analysis of sensor signals for tool condition monitoring: A review and some new results. International Journal of Machine Tools and Manufacture 2009; 49(7): 537-553.

[4] Shao H, Shi X, Li L. Power signal separation in milling process based on wavelet transform and independent component analysis. International Journal of Machine Tools and Manufacture 2011, 51(9): 701-710.

[5] Miner MA. Cumulative damage in fatigue. Applied Mechanics 1945; 12: 159-164.

[6] Palmgren A. Lifetime of ball bearing (in German). VDI-Z 1924; 68: 339-341.

[7] Henry DL. A theory of fatigue-damage accumulation in steel. Trans. of the ASME 1955; 77: 913-918.

[8] Marco SM, Starkley WL. A concept of fatigue damage. Trans. of the ASME 1945; 76: 627-632.

[9] Reddy GRL, Tolbert LM, Ozpineci B, Pinto JO. Rainflow Algorithm-Based Lifetime Estimation of Power Semiconductors in Utility Applications. Trans. on Industry Applications 2015; 51(4): 3368-3375.

[10] Singleton RK, Strangas EG, Aviyente S. Extended Kalman filtering for remaining-useful-life estimation of bearings. Trans. on Industrial Electronics 2015; 62(3): 1781-1790.

[11] Pecht M, Jaai R. A prognostics and health management roadmap for information and electronics-rich systems. Microelectronics Reliability 2010; 50(3): 317-323.

[12] Le Son K, Fouladirad M, Barros A, Levrat E, Iung, B. Remaining useful life estimation based on stochastic deterioration models: A comparative study. Reliability Engineering & System Safety 2013; 112: 165-175.

[13] NASA Prognostics Data Challenge, https://c3.nasa.gov/dashlink/projects/15/. Access date: 01.06.2016.

[14] Si XS, Wang W, Hu CH, Zhou, DH. Remaining useful life estimation - a review on the statistical data driven approaches. European Journal of Operational Research 2011, 213(1): 1-14.

[15] Wang D, Miao Q, Zhou Q, Zhou G. An intelligent prognostic system for gear performance degradation assessment and remaining useful life estimation. Journal of Vibration and Acoustics 2015; 137(2): 1-12.

[16] Baccar D, Söffker D. Wear Detection by Means of Wavelet-based Acoustic Emission Analysis. Mechanical Systems and Signal Processing 2015; 60-61: 198-207.

[17] Söffker D, Schiffer S, Aljouma H, Bacar D. Smart, tough, and successful: Three new innovative approaches for diagnosis and prognosis of technical systems. In: Chang, FK (Ed.): Structural Health Monitoring 2013; 81-88.

[18] Holmberg K, Laukkanen A, Ronkainen H, Waudby R, Stachowiak G, Wolski M, et al. Topographical orientation effects on friction and wear

in sliding DLC and steel contacts, Part 1: Experimental. Wear 2015; 330: 3-22.

[19] Bader N, Pape F, Gatzen HH, Poll G. Examination of friction and wear of a 100Cr6 ball against a bearing ring in a micro-pin-on-disk tester. Surface Effects and Contact Mechanics including Tribology XII: Computational Methods and Experiments 2015, 91:47-55.

[20] Botvina LR, Levin VP, Tyutin MR, Zharkova, NA, Morozov AV, Ozerskii ON, Dobatkin SV. Wear mechanisms of structural steels and effect of wear on their mechanical and acoustic properties during tension. Journal of Friction and Wear 2013; 34(1): 6-13.

[21] Ukpai JI, Barker R, Hu X, Neville A. Exploring the erosive wear of X65 carbon steel by acoustic emission method. Wear 2013; 301(1): 370-382.

[22] Sreenilayam-Raveendran RK, Azarian MH, Morillo C, Pecht MG, Kida K, et al. Comparative evaluation of metal and polymer ball bearings. Wear 2013; 302(1): 1499-1505.

[23] Behrens BA, Bouguecha A, Buse C, Wölki K, Santangelo A. Potentials of in situ monitoring of aluminum alloy forging by acoustic emission. Archives of Civil and Mechanical Engineering 2016; 16(4): 724-733.

[24] Song L. http://www.mathworks.com/matlabcentral/fileexchange/31166-ngpm-a-nsga-ii-program-inmatlab-v1-4. Access date: 20.02.2014.

[25] Weng C, Sun J, Peng H. A unified open-circuit-voltage model of lithium-ion batteries for state-of-charge estimation and state-of-health monitoring. Journal of Power Sources 2014; 258: 228-237.